Genes & Diseases (2023) 10, 2233–2236

Available online at www.sciencedirect.com

ScienceDirect

journal homepage: www.keaipublishing.com/en/journals/genes-diseases

RAPID COMMUNICATION

Circulating fibroblasts present neutrophil-like features in severe COVID-19 cases revealed by single-cell landscape analyses

Severe acute respiratory syndrome coronavirus-2 (SARS-CoV-2), which causes coronavirus disease 2019 (COVID-19) and initially infects epithelial cells of the upper respiratory tract, has recently caused a global health emergency and is still a potential threat to humans.[1] Multiple studies have suggested alterations in the immune system, including excessive neutrophil activation and lymphopenia, and excessive inflammatory responses as the key mechanisms for severe symptoms.[2] However, which cell types contribute to excessive inflammation remains to be explored. Further analysis of human blood immune cells provides insights into the coordinated response to SARS-CoV-2 infections and is a significant task for restraining the virus and controlling disease progression. In this study, we reanalyzed the single-cell sequencing (scRNA-seq) dataset GSE157789 uploaded by Sinha S et al in the GEO database, and the results were validated by analyzing the RNA-seq dataset GSE171110. The results indicated increased neutrophils and plasma cells but reduced CD8 T cells. More importantly, we identified a unique population of fibroblasts enriched in severe COVID-19. The fibroblast subcluster showed potential neutrophil-like function and might be another significant cell population participating in uncontrolled inflammation in COVID-19.

In the analyzed cohort, scRNA-seq was performed using peripheral blood cells from healthy people and severe COVID-19 patients. In total, we sequenced 42,206 cells and 20,737 genes, thereby identifying 16 orthogonal clusters annotated into 11 distinct cell types, namely, CD4 T cells ($CD4^+$), CD8 T cells ($CD8A^+$, $CD8B^+$), B cells ($CD79A^+$, $MS4A1^+$), NK cells ($GNLY^+$, $NKG7^+$), $CD14^+$ monocytes ($CD14^+$ Mono, $CD14^+$, LYZ^+, $FCN1^+$), $CD16^+$ monocytes ($CD16^+$ Mono, $FCGR3A^+$/$CD16^+$), plasma cells ($IGKC^+$, $IGHG1^+$, $JCHAIN^+$), γδT cells ($TRGC2^+$, $GZMA^+$), neutrophils ($FCGR3B^+$), and fibroblasts ($SPARC^+$). Notably, the severe COVID-19 cohort presented a unique landscape of peripheral blood cells with increased neutrophils, plasma cells/B cells, and fibroblasts, and reduced CD8 T cells compared with healthy controls, which was validated by analyzing the RNA-seq data from the GSE171110 dataset performed using peripheral blood from 6 healthy people and 17 severe COVID-19 patient samples (Fig. 1A, B; Fig. S1, 2).

Furthermore, we explored the potential causes of immune cell alterations. The results in Figure S3 indicated that changes in the cell cycle and apoptosis were not responsible for the reduction in CD8 T cells. However, T-cell exhaustion markers, including T-cell immunoglobulin and mucin domain-containing protein 3 (TIM3), lymphocyte activation gene 3 (LAG3), and cytotoxic T-lymphocyte associated protein 4 (CTLA4), were increased in COVID-19 CD8 T cells, which may induce a decrease in CD8 T cells. Increased plasma cells and neutrophils in COVID-19 could be the result of enhanced proliferative activity reflected by the robust G2M cell cycle scores and up-regulation of some cell cycle-related genes (Fig. S4, 5). Notably, the increased chemokines and Toll-like receptors in COVID-19 neutrophils suggested strong chemotaxis and activation (Fig. S5D). Taken together, our analysis results revealed the proinflammatory environment and hyperactive humoral immunity but poor T-cell-mediated antiviral immunity in the peripheral blood of severe COVID-19 patients.

In addition to the deviations in immune cells, the fibroblast population has been found to be increased in severe COVID-19 patients. Reportedly, in COVID-19, this infection may cause the proliferation of fibroblasts and extracellular matrix overproduction. Fibroblasts produce cytokines and cause T-cell infiltration, which may increase

Peer review under responsibility of Chongqing Medical University.

https://doi.org/10.1016/j.gendis.2023.02.032

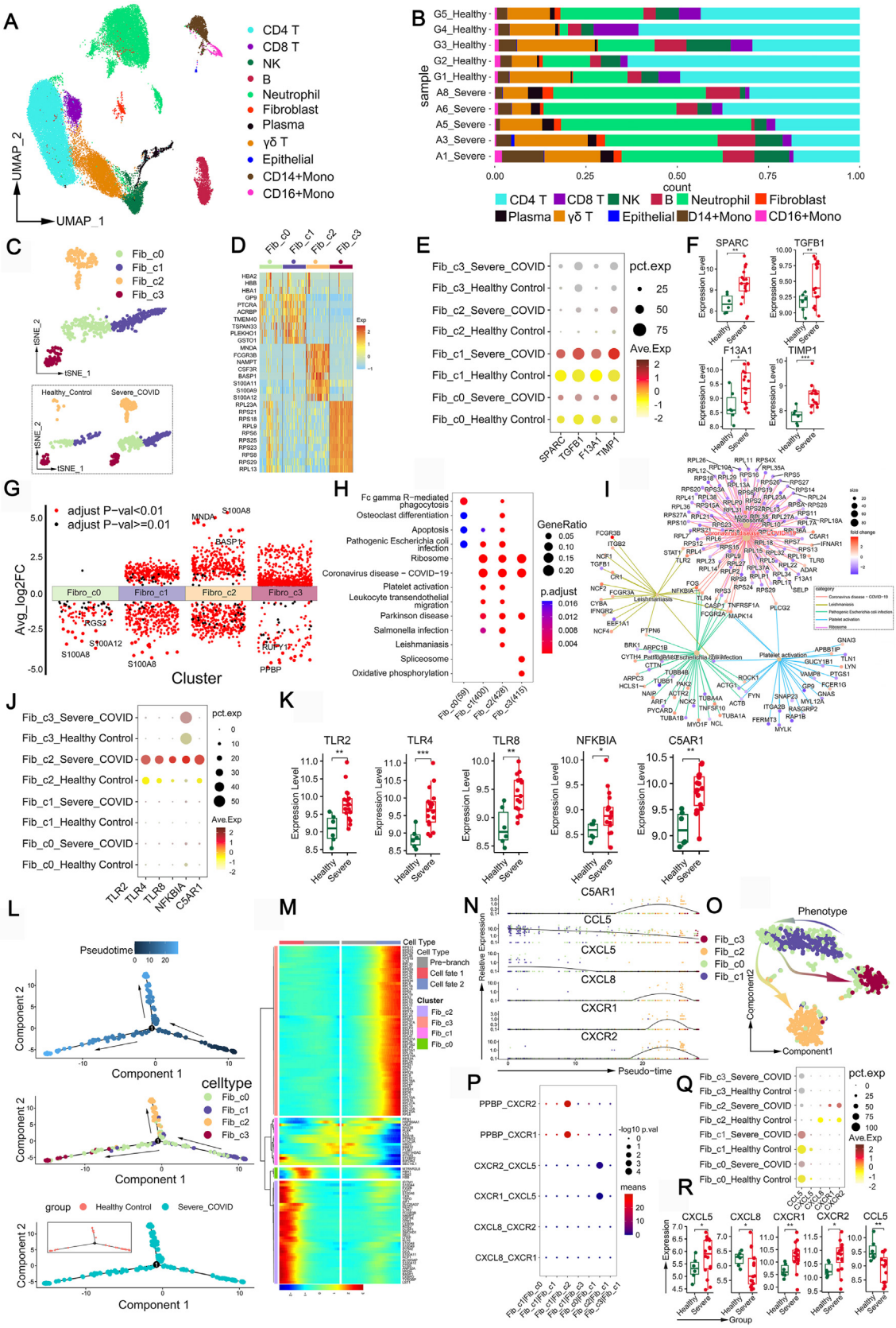

Figure 1 scRNA-seq profiling of the circulating fibroblast populations from healthy people and severe COVID-19 patients. **(A)** The UMAP plots showing the landscape of cell types from healthy people and severe COVID-19 patients. **(B)** The bar plots showing the cell proportions in all samples. **(C)** tSNE projections of subclustered fibroblasts. **(D)** The heatmap indicating the expression of selected gene sets in fibroblast subtypes. **(E)** The dot plots illustrating the expression of nonclassical fibroblasts expressing

inflammation in the lung.[3,4] To decipher the distinctive features of fibroblasts, we identified 4 orthogonal clusters of cells, Fib_c0, Fib_c1, Fib_c2, and Fib_c3 (Fig. 1C). Fib_c0 expressed peripheral erythrocyte-like markers. Fib_c1 expressed high levels of glycoprotein IX platelet (GP9) and transmembrane protein 40 (TMEM40). Fib_c2, which was obviously enriched in the COVID-19 group, showed specific expression of the neutrophil marker genes Fc gamma receptor III b (FCGR3B), S100 calcium-binding protein A8/A9 (S100A8/A9), and colony-stimulating factor 3 receptor (CSF3R), suggesting its potential neutrophil-like function. Fib_c3 expressed high levels of ribosomal protein S21 (RPS21) and ribosomal protein L9 (RPL9) (Fig. 1D). Among fibroblast subclusters, Fib_c1 was a mature type of fibroblast because of the increased expression levels of the profibrotic genes SPARC (secreted protein acidic and rich in cysteine), TIMP1 (TIMP metallopeptidase inhibitor 1), and F13A1 (coagulation factor XIII a chain)[5] (Fig. 1E). This increased fibroblast population in severe COVID-19 patients was validated by analyzing the RNA-seq datasets (Fig. 1F).

Thereafter, differentially expressed gene (DEG) analysis between fibroblast subclusters was performed and is illustrated in Figure 1G. Using these DEGs, we then conducted the Kyoto Encyclopedia of Genes and Genomes (KEGG) analysis between clinical groups. The KEGG pathway analysis indicated that signaling pathways involved in COVID-19, ribosome, and platelet activation were enriched in Fib_c1 and Fib_c2 (Fig. 1H). Due to the neutrophil-like feature of Fib_c2 and its potential proinflammatory capacity, DEGs in subcluster Fib_c2 were selected to redraw KEGG pathways to identify unique functional proteins contributing to the COVID-19 pathway, and the prominent result showed that TLR2, TLR4, TLR8, NFKB inhibitor alpha (NFKBIA) and complement C5a receptor 1 (C5AR1) in COVID-19 pathways were highly expressed in the severe COVID-19 group, exhibiting high pathway activity for the inflammatory response, possibly mediated by Fib_c2 (Fig. 1I, J). The expression pattern was also supported by the analysis of RNA-seq datasets (Fig. 1K). Interestingly, some platelet function-related genes were found to be increased in Fib_c1 from the severe COVID-19 patient group (Fig. S6A, B). The gene set variation analysis (GSVA) pathway analysis also showed high expression scores for coagulation and inflammatory response of fibroblasts (Fig. S6C, D).

We next explored the dynamic cell status and cell transitions in SARS-CoV-2-related fibroblasts by inferring the state trajectories using Monocle 2. According to the lineage relationships and the corresponding gene expression, we performed pseudotime analysis on the merged cells to construct a new trajectory containing two termini corresponding to two distinct cell fates using computational methods BEAM. Fib_c1 cells were found at the start point of the trajectory and then split into two main branches, Fib_c2 cells with partial Fib_c0 cells in fate 1 branch and Fib_c3 cells in fate 2 branch, placed at opposite divergent ends as two terminally differentiated cell types (Fig. 1L, M). The expression levels of selected genes, including C5AR1, CCL5, CXCL5, CXCL8, CXCR1, and CXCR2, along with the pseudotime showed dynamic changes in inflammatory responses, including neutrophil recruitment and neutrophil-related inflammation (Fig. 1N). The expression levels of C5AR1, CXCL8, CXCR1, and CXCR2 were extremely low along with the pseudotime until reaching the fate 1 branch (mainly Fib_c2) and declined again when reaching the fate 2 branch (Fib_c3), suggesting the potential neutrophil-like function of Fib_c2. The expression levels of CCL5 and CXCL5 were high in Fib_c1 and decreased gradually along with the pseudotime. The results indicated the chemotaxis potential of Fib_c1 to neutrophils or neutrophil-like cells, such as Fib_c2. Consistently, our results were further validated by another analysis strategy, CytoTRACE (Fig. 1O). To determine the possible communications among heterogeneous fibroblasts, we performed ligand/receptor/target gene coexpression analysis using the CellPhoneDB algorithm. The results indicated that Fib_c0 primarily interacted with itself and Fib_c2. In our data, the receiver cell Fib_c2 with high levels of CXCR1 and CXCR2 can be strongly predicted to interact with the sender cell Fib_c1 through CXCL5 (Fig. 1P; Fig. S6E). These identified ligands and their downstream targets might also be responsible for the

complement transcripts SPARC, TGFB1, F13A1, and TIMP1 between healthy people and severe COVID-19 patients. **(F)** The boxplots showing the expression of selected genes SPARC, TGFB1, F13A1, and TIMP1. The data was searched from the GEO database. Paired or unpaired Wilcoxon tests were used for all statistical analyses; $^{*}P < 0.05$, $^{**}P < 0.01$, $^{***}P < 0.001$. **(G)** The volcano plot showing the differentially expressed genes of four clusters. Black dots indicate non-significantly different genes, and red dots indicate significantly different genes. **(H)** The dot plots showing KEGG biological process terms enriched in cluster marker genes. **(I)** The network showing the dynamic changes in expression along the subset fibroblasts cluster 2 (Fib_2). **(J)** The dot plots illustrating the expression and cell proportion of selected genes TLR2, TLR4, TLR8, NFKBIA, and C5AR1 in different subclusters between healthy people and severe COVID-19 patients. **(K)** The boxplots showing the expression of selected genes TLR2, TLR4, TLR8, NFKBIA, and C5AR1. The data was searched from the GEO database. Paired or unpaired Wilcoxon tests were used for all statistical analyses; $^{*}P < 0.05$, $^{**}P < 0.01$, $^{***}P < 0.001$. **(L)** Pseudotime-ordered analysis of subclusters of fibroblasts displayed by clustering and color-coding according to cell type or clinical group. **(M)** The heatmap revealing the dynamic changes in gene expression during the differentiation process. The distribution of fibroblast subtypes during the transition was divided into four phases, along with the pseudotime. **(N)** The dot plots showing the dynamic changes in selected gene expression along with the pseudotime. **(O)** The two-dimensional plots showing the expression scores for genes in another algorithm CytoTRACE in healthy people and severe COVID-19 samples, along with the pseudotime. **(P)** The dot plot showing the selected significant receptor−ligand interactions between subset fibroblast cells discovered using CellPhoneDB (empirical permutation *P* value). **(Q)** The dot plots illustrating the expression and cell proportion of selected genes CCL5, CXCL5, CXCL8, CXCR1, and CXCR2 in different subclusters between healthy people and severe COVID-19 patients. **(R)** The box plots showing the expression of selected marker genes in the clinical group between healthy people and severe COVID-19 patients. The data was searched from the GEO database. Paired or unpaired Wilcoxon tests were used for all statistical analyses; $^{*}P < 0.05$, $^{**}P < 0.01$.

inflammation-associated phenotype of neutrophils. Moreover, in scRNA-seq data of fibroblasts, the expression levels of CXCL5 in Fib_c1 and CXCL8, CXCR1 and CXCR2 in Fib_c2 were much higher in severe COVID-19 patients (Fig. 1Q). These results were validated by analyzing the RNA-seq datasets (Fig. 1R). Furthermore, we found enhanced expression levels of inflammatory response-related transcription factors by using the ChEA3 tool (Fig. S6F), suggesting that fibroblasts contributed to the enhanced proinflammatory neutrophil microenvironment in patients with severe COVID-19.

To summarize, our study revealed the features of circulating immune cells and identified a significant fibroblast population with neutrophil-like function participating in uncontrolled inflammation in COVID-19.

Conflict of interests

The authors have no potential conflict of interests to disclose.

Appendix A. Supplementary data

Supplementary data to this article can be found online at https://doi.org/10.1016/j.gendis.2023.02.032.

References

1. Morens DM, Fauci AS. Emerging pandemic diseases: how we got to COVID-19. *Cell*. 2020;182(5):1077–1092.
2. Wang X, Gui J. Cell-mediated immunity to SARS-CoV-2. *Pediatr Investig*. 2020;4(4):281–291.
3. Sahin M, Akkus E. Fibroblast function in COVID-19. *Pathol Res Pract*. 2021;219:153353.
4. John AE, Joseph C, Jenkins G, et al. COVID-19 and pulmonary fibrosis: a potential role for lung epithelial cells and fibroblasts. *Immunol Rev*. 2021;302(1):228–240.
5. Shieh DH, Chiang LC, Shieh TY. Augmented mRNA expression of tissue inhibitor of metalloproteinase-1 in buccal mucosal fibroblasts by arecoline and safrole as a possible pathogenesis for oral submucous fibrosis. *Oral Oncol*. 2003;39(7):728–735.

Xiangjun Liu, Jingang Gui, Xiaolin Wang *

Laboratory of Tumor Immunology, Beijing Pediatric Research Institute, Beijing Children's Hospital, Capital Medical University, National Center for Children's Health (NCCH), Beijing 100045, China

*Corresponding author.
E-mail address: wangxl19891012@163.com (X. Wang)

16 December 2022
Available online 27 March 2023